Dyes and Pigments 85 (2010) 79–85

Contents lists available at ScienceDirect

Dyes and Pigments

journal homepage: www.elsevier.com/locate/dyepig

Pyrazolyl-substituted polyconjugated molecules for optoelectronic applications

E. Arbačiauskienė [a], K. Kazlauskas [b,*], A. Miasojedovas [b], S. Juršėnas [b], V. Jankauskas [c], W. Holzer [d], V. Getautis [a], A. Šačkus [a,**]

[a] Department of Organic Chemistry, Kaunas University of Technology, Radvilėnų pl. 19, LT-50270, Kaunas, Lithuania
[b] Institute of Applied Research, Vilnius University, Saulėtekio 9-III, LT-10222, Vilnius, Lithuania
[c] Department of Solid State Electronics, Vilnius University, Saulėtekio 9-III, LT-10222, Vilnius, Lithuania
[d] Department of Drug and Natural Product Synthesis, Faculty of Life Sciences, University of Vienna, Althanstrasse 14, A-1090 Vienna, Austria

ARTICLE INFO

Article history:
Received 17 June 2009
Received in revised form
13 October 2009
Accepted 17 October 2009
Available online 28 October 2009

Keywords:
Pyrazole
Cyano groups
Fluorescence
Ionization potential
Charge carrier mobility

ABSTRACT

Pyrazolyl-substituted diethylene derivative and its analogue containing additional cyano groups were synthesized and investigated as potential multifunctional materials for organic light emitting diodes. The influence of the electron affinitive cyano groups on the ionization potential (I_p) of the films as well as on the photoluminescence (PL) spectrum, PL quantum yield (η) and PL decay time of the dilute solutions and thin films of the pyrazole derivatives was studied. PL measurements revealed that highly luminescent ($\eta = 0.88$) cyano-free pyrazole derivative in solution became non-emissive ($\eta = 0.01$) by attaching cyano groups as a result of these groups-induced torsional deactivation. However in the solid state, the steric and electrostatic effects of the bulky and polar cyano groups prevented tight packing of the pyrazole derivative molecules, thus significantly reducing migration-induced quenching of the excitons at the defects. Incorporation of the cyano groups resulted in the two-fold enhancement of the PL quantum yield in the film of the pyrazole derivative as compared to that of the cyano-free film. The I_p of 5.90 eV estimated for the cyano groups-containing compound was found to be higher as compared to the I_p of 5.46 eV for cyano-free analogue, what in conjunction with the PL data for the films indicates increased electron affinity in the pyrazole derivative with additional cyano groups.

1. Introduction

Low-molecular-weight functional dyes exhibiting both emission and charge transport are of interest for the application in optoelectronic devices such as organic light emitting diodes (OLEDs) [1]. Although much progress has been achieved on OLEDs, there are still some challenges of improving the performance and durability of OLEDs for displays and lighting applications. One of the key issues for developing the next generation high-performance OLEDs is the design and synthesis of multifunctional materials with both light emission and charge transport properties. The molecules consisting of polyconjugated structure end-capped with heteroaromatic or polycyclic aromatic chromophores are known to be highly fluorescent [2–4]. Vinylene linkage that is often employed in the design of the polyconjugated molecules serve not only as a “conjugated bridge”, it also improves electroluminescent properties by reducing steric interactions between aromatic rings, and thus, decreasing the free rotation between units [5]. Pyrazoline derivatives are known to exhibit efficient blue emission and hole-transport performance, and therefore, might serve as the multifunctional materials for light emitting devices [6]. As distinct from pyrazoline, aromatic pyrazole is much less studied and exploited as electroactive moiety.

Introduction of cyano groups into the vinylene linkages of the polyconjugated materials has an advantage of increasing electron affinity, and therefore, greatly improving electron injection from the metal contact of an OLED [7]. Incorporation of cyano moieties into fluorescent compounds also facilitates formation of highly fluorescent organic nanoparticles, which have potential applications in on/off fluorescence sensors [8].

To this end, pyrazolyl-substituted diethylene derivative 1,4-bis{(*E*)-2-[(1-biphenylyl-3-hexyloxy)pyrazol-4-yl]ethenyl}benzene (**P1**) and its analogue with cyano moieties 1,4-bis{(*E*)-1-nitrile-2-[(1-biphenylyl-3-hexyloxy)pyrazol-4-yl]ethenyl}benzene (**P2**) have been synthesized and characterized. Here, the photophysical and

---

* Corresponding author. Tel.: +370 52 366032; fax: +370 52 366059.
** Corresponding author. Tel.: +370 37 300194; fax: +370 37 451432.
E-mail addresses: karolis.kazlauskas@ff.vu.lt (K. Kazlauskas), algirdas.sackus@ktu.lt (A. Šačkus).

0143-7208/$ – see front matter © 2009 Elsevier Ltd. All rights reserved.
doi:10.1016/j.dyepig.2009.10.007

photoelectrical properties of the synthesized pyrazole derivatives are reported.

2. Experimental details

2.1. Measurements

The ^{1}H and ^{13}C NMR spectra were measured on Varian Unity Inova spectrometer (^{1}H–300 MHz, ^{13}C–75 MHz) or on Bruker Avance 500 spectrometer (^{1}H–500 MHz, ^{13}C–125 MHz) in $CDCl_3$. The IR spectra of the samples in KBr pellets were recorded on a Perkin Elmer Spectrum GX FT-IR System spectrometer. The absorption spectra of the sample THF solutions (10^{-4} M) placed in a 1 mm path length microcell were recorded on a Perkin Elmer Lambda 35 UV/VIS spectrometer. Photoluminescence (PL) of the sample solutions and thin films was excited by 365 nm wavelength light emitting diode (Nichia NSHU590-B) and measured using back-thinned CCD spectrometer (Hamamatsu PMA-11). The luminescence quantum yield (η) of the solutions was estimated by comparing wavelength-integrated PL intensity of the solution with that of the reference. Quinine sulfate dissolved in 0.1 M H_2SO_4 and exhibiting $\eta = 53 \pm 2.3\%$ at an excitation wavelength of 366 nm has been used as a reference [9]. Optical densities of the reference and the sample solutions were ensured to be below 0.05 to avoid reabsorption effects. Estimated quantum yield was verified by using an alternative method of an integrating sphere (Sphere Optics) coupled to the CCD spectrometer [10]. The integrated sphere method was also employed in the quantum yield estimations of the thin films. PL transients of the sample solutions and thin films were measured using time-correlated single photon counting system (PicoQuant PicoHarp 300). Pulsed excitation at 1 MHz repetition rate was provided by picosecond diode laser with the pulse duration of 70 ps and the emission wavelength of 375 nm.

The ionization potentials (I_p) of the sample films were estimated by performing electron photoemission spectroscopy (PES) in air, as it is described in Refs. [11,12]. The charge carrier mobilities were measured by the xerographic time-of-flight technique (XTOF) [13,14]. The samples for the mobility measurements were prepared by casting the materials dispersed in bisphenol Z polycarbonate (PC-Z) (Iupilon Z-200 from Mitsubishi Gas Chemical Co.) on polyester film with conductive Al layer serving as the sample substrate. In XTOF measurements, the electric field inside the sample was created by applying positive corona charging. Charge carriers at the sample surface were generated by exciting the sample with the pulses of nitrogen laser (pulse duration 1 ns, wavelength 337 nm). Excitation induced decrease of the surface potential by 1–5% was achieved in respect of the initial potential before excitation. The capacitance probe connected to a wide-frequency-band electrometer was employed to monitor the time evolution of the surface potential decrease rate dU/dt after the excitation, which was used to extract charge carrier transit time, and consequently, to deduce carrier drift mobility (μ).

The course of the reactions was monitored by TLC on Merck TLC aluminium Silica gel 60 F_{254} sheets and developed with I_2 or UV light. Silica gel (Merck, grade 9385, 230–400 mesh, pore size 60 Å) was used for column chromatography. Elemental analyses were performed with an Exeter Analytical CE-440 Elemental Analyzer. Melting points were determined in capillary tubes on capillary melting point apparatus Electrothermal MEL-TEMP®.

2.2. Materials

4-Bromo-1-(4-bromophenyl)-3-hydroxy-1H-pyrazole (**3**) was synthesized according the procedure described in Ref. [15].

2.2.1. 4-Bromo-1-(4-bromophenyl)-3-hexyloxy-1H-pyrazole (*4*, $C_{15}H_{18}Br_2N_2O$)

The solution of **3** (2.23 g, 7 mmol) in dry DMF (20 ml) was cooled to 0 °C under inert atmosphere and NaH (60% dispersion in mineral oil, 280 mg, 7 mmol) was added portion wise. After mixing for 15 min hexyl bromide (1.2 ml, 8.4 mmol) was added drop wise. The mixture was stirred at 60 °C for 3 h (TLC control, eluent: ethyl acetate:*n*-hexane = 1:10). 10 ml of water were added and the mixture was extracted with ethyl acetate. The organic layers were combined, washed with brine, dried over Na_2SO_4, filtrated, the solvent was evaporated. The residue was purified by column chromatography (eluent: ethyl acetate:*n*-hexane = 1:10) to give pure **4** as a liquid. Yield: 95% (2.67 g); IR (KBr; ν, cm^{-1}): 3143 (CH_{arom}), 2954, 2930, 2858 (CH_{aliph}), 1593, 1549, 1512, 1494, 1470, 1424, 1392, 1368, 1309 (C═C, C–N), 1219, 1098 (C–O–C), 824 (CH ═ CH of disubstituted benzene); ^{1}H NMR (300 MHz, $CDCl_3$; δ, ppm): 7.74 (s, 1H, 5-H), 7.54–7.50 (m, 2H, Ph 2,6-H), 7.45–7.41 (m, 2H, Ph 3,5-H), 4.30 (t, $J = 6.6$ Hz, 2H, OCH_2), 1.87–1.78 (m, 2H, $OCH_2C\underline{H_2}$), 1.51–1.42 (m, 2H, $O(CH_2)_2C\underline{H_2}$), 1.40–1.32 (m, 4H, $(C\underline{H_2})_2CH_3$), 0.91 (t, $J = 7.0$ Hz, 3H, CH_3); ^{13}C NMR (75 MHz, $CDCl_3$; δ, ppm): 161.01 (C-3), 138.73 (Ph C-1), 132.80 (Ph C-3,5), 127.39 (C-5), 118.87 (Ph C-2,6), 118.55 (Ph C-4), 83.18 (C-4), 69.86 (OCH_2), 31.47 ($\underline{C}H_2CH_2CH_3$), 28.92 ($OCH_2\underline{C}H_2$), 25.49 ($OCH_2CH_2\underline{C}H_2$), 22.58 ($\underline{C}H_2CH_3$), 14.02 ($CH_3$). APCI-MS: *m/z* (%) = 405 $[M + H + 4]^+$ (48), 403 $[M + H + 2]^+$ (100), 401 $[M + H]^+$ (48); Anal. Calcd for $C_{15}H_{18}Br_2N_2O$: C, 44.80; H, 4.51; N, 6.97. Found, %: C, 44.40; H, 4.06; N, 6.72.

2.2.2. 1-(4-Bromophenyl)-3-hexyloxy-1H-pyrazole-4-carbaldehyde (*5*, $C_{16}H_{19}BrN_2O_2$)

To a solution of **4** (804 mg, 2 mmol) in 16 ml of absolute THF under inert atmosphere at −78 °C *n*-BuLi (2.5 M in hexane, 0.8 ml, 2 mmol) was added drop wise and dry DMF (0.23 ml, 3 mmol) was added. The mixture was gradually warmed up to room temperature and stirred for 30 min (TLC control, eluent: ethyl acetate:*n*-hexane = 1:10). 5 ml of water were added and extraction was done with ethyl acetate. The organic layers were combined, washed with brine, dried over Na_2SO_4, filtrated, the solvent was evaporated. The residue was purified by column chromatography (eluent: ethyl acetate:*n*-hexane = 1:10) to give pure **5** as a liquid. Yield: 50% (351 mg); IR (KBr; ν, cm^{-1}): 3127, 3101 (CH_{arom}), 2955, 2930, 2857 (CH_{aliph}), 1669 (C═O), 1562, 1508, 1374, (C═C, C–N), 1224, 1209 (C–O–C), 821 (CH ═ CH of disubstituted benzene); ^{1}H NMR (300 MHz, $CDCl_3$; δ, ppm): 9.85 (s, 1H, CHO), 8.21 (s, 1H, 5-H), 7.59–7.50 (m, 4H, Ph-H), 4.37 (t, $J = 6.6$ Hz, 2H, $OC\underline{H_2}$), 1.89–1.80 (m, 2H, $OCH_2C\underline{H_2}$), 1.52–1.43 (m, 2H, $O(CH_2)_2C\underline{H_2}$), 1.38–1.33 (m, 4H, $O(CH_2)_3(C\underline{H_2})_2$), 0.91 (t, $J = 7.0$ Hz, 3H, CH_3); ^{13}C NMR (75 MHz, $CDCl_3$; δ, ppm): 183.33 ($\underline{C}HO$), 164.03 (C-3), 137.98 (Ph C-1), 132.54 (Ph C-3,5), 129.01 (C-5), 120.36 (Ph C-4), 120.07 (Ph C-2,6), 111.68 (C-4), 69.70 ($O\underline{C}H_2$), 31.45 ($\underline{C}H_2CH_2CH_3$), **28.83** ($OCH_2\underline{C}H_2$), 25.49 ($OCH_2CH_2\underline{C}H_2$), 22.51 ($\underline{C}H_2CH_3$), 13.99 ($CH_3$); APCI-MS: *m/z* (%) = 375 $[M + Na + 2]^+$ (47), 373 $[M + Na]^+$ (48), 295 $[M\text{-}Br + Na]^+$ (100); Anal. Calcd for $C_{15}H_{18}Br_2N_2O$: C, 44.80; H, 4.51; N, 6.97. Found, %: C, 55.11; H, 5.81; N, 8.07.

2.2.3. 1-(Biphenyl-4-yl)-3-hexyloxy-1H-pyrazole-4-carbaldehyde (*6*, $C_{22}H_{24}N_2O_2$)

To a solution of pyrazole **5** (350 mg, 1 mmol) in 1,4-dioxane (10 ml) under argon atmosphere anhydrous K_3PO_4 (636 mg, 3 mmol), phenylboronic acid (366 mg, 3 mmol) and $Pd(PPh_3)_4$ (92 mg, 0.08 mmol) were added. After refluxing for 3 h under argon atmosphere (TLC control, eluent: ethyl acetate:*n*-hexane = 1:10) the mixture was diluted with water (10 ml) and extracted with ethyl acetate. The combined organic layers were washed with brine, dried over sodium sulfate, filtrated, the solvent was evaporated. The product was purified by column chromatography (eluent: ethyl acetate:*n*-hexane = 1:20) to give **6** as a liquid. Yield 94% (327 mg), IR (KBr; ν, cm^{-1}): 3119, 3087 (CH_{arom}), 2954, 2934, 2850 (CH_{aliph}), 1674 (C═O), 1563, 1499, 1367, 1354 (C═C, C–N), 1222, 1202 (C–O–C), 840, 768, 701 (CH = CH of mono- and disubstituted benzenes); ^{1}H NMR (300 MHz, $CDCl_3$; δ, ppm): 9.87 (s, 1H, CHO), 8.28 (s, 1H, 5-H), 7.73–7.66 (m, 4H, N-Ph-H), 7.61–7.59 (m, 2H, N-Ph-Ph 2,6-H), 7.49–7.44 (m, 2H, N-Ph-Ph 3,5-H), 7.40–7.38 (N-Ph-Ph 4-H), 4.41 (t, *J* = 6.6 Hz, 2H, $OC\underline{H_2}$), 1.87 (m, 2H, $OCH_2C\underline{H_2}$), 1.55–1.45 (m, 2H, $O(CH_2)_2C\underline{H_2}$), 1.40–1.35 (m, 4H, $O(CH_2)_3(C\underline{H_2})_2$), 0.94 (t, *J* = 7.0 Hz, 3H, CH_3); ^{13}C NMR (75 MHz, $CDCl_3$; δ, ppm): 183.39 ($\underline{C}HO$), 164.12 (C-3), 140.08, 139.77, 138.18, 129.04, 128.88, 128.14, 127.68, 126.86, 119.04 (Ph C-2,6), 111.52 (C-4), 69.70 ($O\underline{C}H_2$), 31.48($\underline{C}H_2CH_2CH_3$), 28.93 ($OCH_2\underline{C}H_2$), 25.56 ($OCH_2CH_2\underline{C}H_2$), 22.54 ($\underline{C}H_2CH_3$), 14.00 ($CH_3$); APCI-MS: *m/z* (%) = 371 $[M + Na]^+$ (100); Anal. Calcd for $4C_{15}H_{18}Br_2N_2O*3H_2O$: C, 73.00; H, 7.10; N, 7.74. Found, %: C, 72.80; H, 6.94; N, 7.52.

2.2.4. 1,4-Bis{(E)-2-[(1-biphenylyl-3-hexyloxy)pyrazol-4-yl] ethenyl}benzene (P1, $C_{52}H_{54}N_4O_2$)

To the suspension of **6** (348 mg, 1 mmol) and [1,4-phenylenebis(methylen)]-bis[triphenylphosphonium] dibromide (315 mg, 0.4 mmol) in abs. THF (10 ml) under argon atmosphere NaOMe (408 mg, 6 mmol) solution in abs. MeOH (8 ml) was added. Reaction mixture was stirred overnight at r.t. under argon atmosphere (TLC control, eluent: dichloromethane:diethyl ether:*n*-hexane = 6:2:16). Reaction mixture was poured into water (15 ml) and extracted with chloroform. The combined organic layers were washed with brine, dried over sodium sulfate, filtrated, the solvent was evaporated. The residue was refluxed with I_2 (25 mg, 0.1 mmol) in 10 ml of chloroform for 30 min. After cooling to room temperature the mixture was washed with sat. $Na_2S_2O_3$ solution. The organic layer was washed with brine, dried over sodium sulfate, filtrated, the solvent was evaporated. The product was crystallized from chloroform: diethyl ether = 1:2. Yield of **P1** was 54% (166 mg), mp 213–218 °C. IR (KBr; ν, cm^{-1}): 3034 (CH_{arom}), 2952, 2927, 2856 (CH_{aliph}), 1607, 1565, 1525, 1491, 1400, 1363, 1356 (C═C, C–N), 1247, 1204 (C–O–C), 837, 762, 696 (CH = CH of mono- and disubstituted benzenes). ^{1}H NMR (500 MHz, $CDCl_3$; δ, ppm): 7.86 (s, 2H, Pyr 3-H), 7.67 (m, 4H, N-Ph 3,5-H), 7.65 (m, 4H, N-Ph 2,6-H), 7.61 (m, 4H, N-Ph-Ph 2,6-H), 7.46 (m, 4H, N-Ph-Ph 3,5-H), 7.44 (s, 4H, CH-Ph-$\underline{H}$), 7.36 (m, 2H, N-Ph-Ph 4-H), 7.14 (d, *J* = 16.3 Hz, 2H, Pyr-CH = C$\underline{H}$), 6.95 (d, *J* = 16.3 Hz, 2H, Pyr-C$\underline{H}$), 4.42 (t, *J* = 6.6 Hz, 4H, $O{-}C\underline{H_2}$), 1.91 (m, 4H, $OCH_2C\underline{H_2}$), 1.57 (m, 4H, $OCH_2CH_2C\underline{H_2}$), 1.42 (m, 4H, $C\underline{H_2}CH_2CH_3$), 1.40 (m, 4H, $C\underline{H_2}CH_3$), 0.95 (t, *J* = 7.0 Hz, 3H, CH_3); ^{13}C NMR (125 MHz, $CDCl_3$; δ, ppm):162.3 (Pyr-C-3), 140.2 (N-Ph-Ph-C-1), 139.1 (N-Ph-C-4), 137.9 (N-Ph-C-1), 136.8 (CH-Ph-C-1,4), 128.8 (N-Ph-Ph-C-3,5), 128.0 (N-Ph-C-2,6), 127.5 (Pyr-4-CH = $\underline{C}$), 127.3 (N-Ph-Ph-C-4), 126.8 (N-Ph-Ph-C-2,6), 126.2 (CH-Ph-$\underline{C}$), 124.7 (Pyr-C-5), 117.7 (N-Ph-C-3,5), 116.6 (Pyr-4-$\underline{C}$H), 108.8 (Pyr-4-C), 69.2 (O–C), 31.7 ($\underline{C}H_2CH_2CH_3$), 29.1 ($OCH_2\underline{C}H_2$), 25.8 ($OCH_2CH_2\underline{C}H_2$), 22.6 ($\underline{C}H_2CH_3$), 14.1 ($CH_3$); APCI-MS: *m/z* (%) = 767 $[M + H]^+$ (50), 451 $[M{-}2 \times C_6H_5{-}C_{11}H_{26}O_2 + Na]^+$, (100); Anal. Calcd for $C_{52}H_{54}N_4O_2 \times H_2O$: C, 79.56; H, 7.17; N, 7.14. Found, %: C, 79.57; H, 7.17; N, 6.90.

2.2.5. 1,4-Bis{(E)-1-nitrile-2-[(1-biphenylyl-3-hexyloxy)pyrazol-4-yl]ethenyl}benzene (P2, $C_{54}H_{52}N_6O_2$)

To the suspension of **6** (348 mg, 1 mmol) and 1,4-phenylenediacetonitrile (63 mg, 0.4 mmol) in dry chloroform (15 ml) and abs. MeOH (4 ml) under argon atmosphere NaOMe (408 mg, 6 mmol) solution in abs. MeOH (4 ml) was added. Reaction mixture was stirred overnight at r.t. under argon atmosphere (TLC control, eluent: dichloromethane:diethyl ether:*n*-hexane = 6:2:16). Reaction mixture was poured into water (15 ml) and extracted with chloroform. The combined organic layers were washed with brine, dried over sodium sulfate, filtrated, the solvent was evaporated. The product was crystallized from chloroform:diethyl ether = 1:2. Yield of **P2** was 45% (147 mg), mp 235–236 °C. IR (KBr; ν, cm^{-1}): 3033 (CH_{arom}), 2953, 2929, 2856 (CH_{aliph}), 2210 (C≡N), 1598, 1562, 1523, 1491, 1467, 1377, 1340 (C═C, C–N), 1229 (C–O–C), 837, 762, 697 (CH = CH of mono- and disubstituted benzenes). ^{1}H NMR (500 MHz, $CDCl_3$; δ, ppm): 8.81 (s, 2H, Pyr-5-H), 7.76 (m, 4H, N-Ph 3,5-H), 7.69 (s, 4H, CH = CH-Ph-$\underline{H}$), 7.68 (m, 4H, N-Ph 2,6-H), 7.62 (m, 4H, N-Ph-Ph 2,6-H), 7.53 (s, 2H, Pyr-C$\underline{H}$), 7.47 (m, 4H, N-Ph-Ph 3,5-H), 7.37 (m, 2H, N-Ph-Ph 4-H), 4.42 (t, *J* = 6.6 Hz, 4H, $O{-}C\underline{H_2}$), 1.89 (m, 4H, $OCH_2C\underline{H_2}$), 1.52 (m, 4H, $OCH_2CH_2C\underline{H_2}$), 1.40 (m, 4H, $C\underline{H_2}CH_2CH_3$), 1.39 (m, 4H, $C\underline{H_2}CH_3$), 0.94 (t, *J* = 7.0 Hz, 6H, CH_3); ^{13}C NMR (125 MHz, $CDCl_3$; δ, ppm):163.6 (Pyr-C-3), 140.0 (N-Ph-Ph-C-1), 139.4 (N-Ph-C-1), 138.5 (N-Ph-C-4), 134.1 (CH-Ph-C-1,4), 130.4 (Pyr-$\underline{C}$H), 128.9 (N-Ph-Ph-C-3,5), 128.1 (N-Ph-C-2,6), 127.6 (N-Ph-Ph-C-4), 127.0 (N-Ph-Ph-C-2,6), 126.4 (Pyr-C-5), 125.8 (C-CN-Ph-C-2,3,5,6), 119.1 (C≡N), 118.8 (N-Ph-C-3,5), 105.7 (Pyr-C-4), 105.6 (C≡N–$\underline{C}$), 69.8 ($O{-}\underline{C}H_2$), 31.6 ($\underline{C}H_2CH_2CH_3$), 29.0 ($OCH_2\underline{C}H_2$), 25.7 ($OCH_2CH_2\underline{C}H_2$), 22.6 ($\underline{C}H_2CH_3$), 14.1 ($CH_3$); APCI-MS: *m/z* (%) 817 $[M + H]^+$ (10), 492 $[M{-}2C_6H_5{-}2CN + H]^+$ (50), 406 $[M{-}2C_6H_5{-}2CN{-}2C_3H_6 + H]^+$ (100); Anal. Calcd for $C_{54}H_{52}N_6O_2 \times 3H_2O$: C, 74.46; H, 6.71; N, 9.65. Found, %: C, 74.45; H, 6.30; N, 9.24.

3. Results and discussion

3.1. Synthesis and characterization

The synthetic strategy (Scheme 1) displays the chemical reaction scheme that was used to synthesize the key compound 1-(biphenyl-4-yl)-3-hexyloxy-1*H*-pyrazole-4-carbaldehyde (**6**) and is based on these concepts.

Thus, dihalopyrazole synthon **3** was prepared via 3-hydroxy-4-phenyl-1*H*-pyrazole (**2**) starting from the commercially available 1-phenylpyrazolidin-3-one following the previously reported

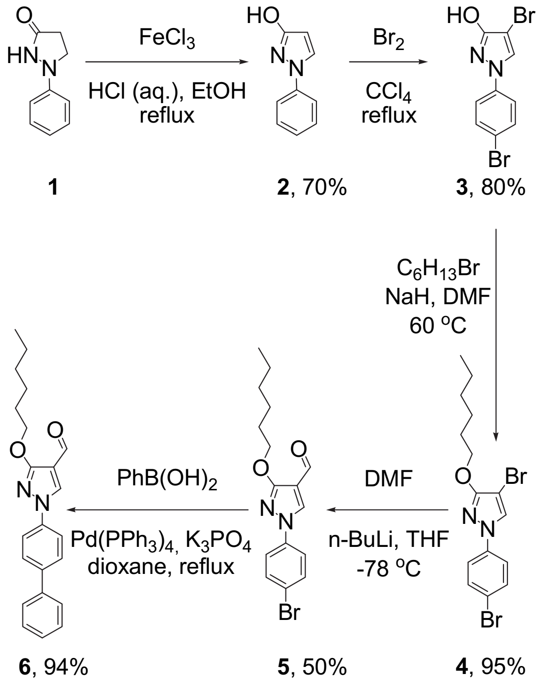

Scheme 1. Synthesis route to 1-(biphenyl-4-yl)-3-hexyloxy-1*H*-pyrazole-4-carbaldehyde (**6**).

methods [15]. Then, the hydroxyl group of **3** was alkylated (hexyloxy group introduction) to lengthen the side chains of target polyconjugated structures **P1** and **P2** for the better solubility. The key step - formylation of intermediate **4** was performed with the addition of 1 equiv of *n*-BuLi (2.5 M solution in hexanes) in THF at −78 °C which was quenched with DMF. As the result only selectively monoformylated pyrazole **5** formed in the reaction mixture. The highest yield of **5** was achieved by rapidly adding *n*-BuLi - and immediately after that quenching with DMF to avoid the decomposition of the formed aryllithium intermediate. The structure of the carbaldehyde **5** was analyzed and identified following the ^{1}H, ^{13}C NMR, IR, MS spectroscopy and elemental analysis data. The ^{1}H NMR spectrum of **5** displays the signal of the aldehyde proton at 9.85 ppm. The ^{13}C NMR spectrum of **5** as compared with the spectrum of **4** displays the additional signal at 183.30 ppm, which belongs to the aldehyde group, while the signal of C-4 at 83.18 ppm in the spectrum of **4** is changed to 111.77 ppm in the spectrum of **5** that prove the selective formylation of the heterocyclic ring to C-4 position (Fig. 1).

To extend the π-conjugated system compound **5** was further coupled with the phenylboronic acid under Suzuki reaction conditions to give the pyrazolecarbaldehyde derivative **6** in a high yield. The target compound **P1** was synthesized using well known Wittig reaction conditions from carbaldehyde **6** and corresponding bis(triphenylphosphonium) salt (Scheme 2). As it was observed from the crude sample of **P1** according to the TLC and ^{1}H NMR spectral data an inseparable mixture of *cis*/*trans*-olefin geometries was formed. The isomers *cis*–*cis* and *cis*-*trans* were converted to the *trans*–*trans* isomer following the previously reported methods [16], as the presences of *cis* isomers are detrimental to the emission properties of polyconjugated molecules [17].

The synthesis of the same skeletal structure **P2**, but consisting of two CN groups, was fulfilled by the Knoevenagel reaction of carbaldehyde **6** and 1,4-phenylenediacetonitrile. We anticipated that the introduction of an additional electron-withdrawing function in this molecule could dramatically affect its properties as a luminescent material.

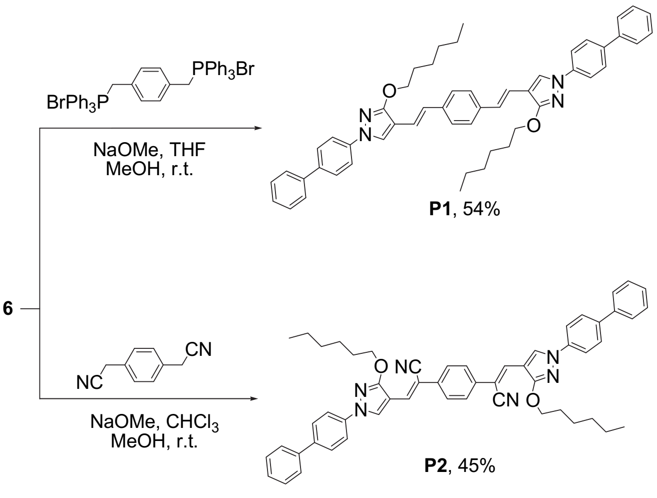

Scheme 2. Synthesis route to the polyconjugated molecules **P1** and **P2**.

The structures of **P1** and **P2** were analyzed and identified following the ^{1}H, ^{13}C NMR, IR, MS spectroscopy and elemental analysis data.

3.2. Photophysical and photoelectrical properties of P1 and P2

Fig. 2 displays absorption and PL spectra of the dilute solutions of compounds **P1** and **P2** and PL spectra of their thin films. The lowest energy absorption bands of the two pyrazolyl-substituted diethylenes **P1** and **P2** in dilute solutions exhibit maxima at 383 nm

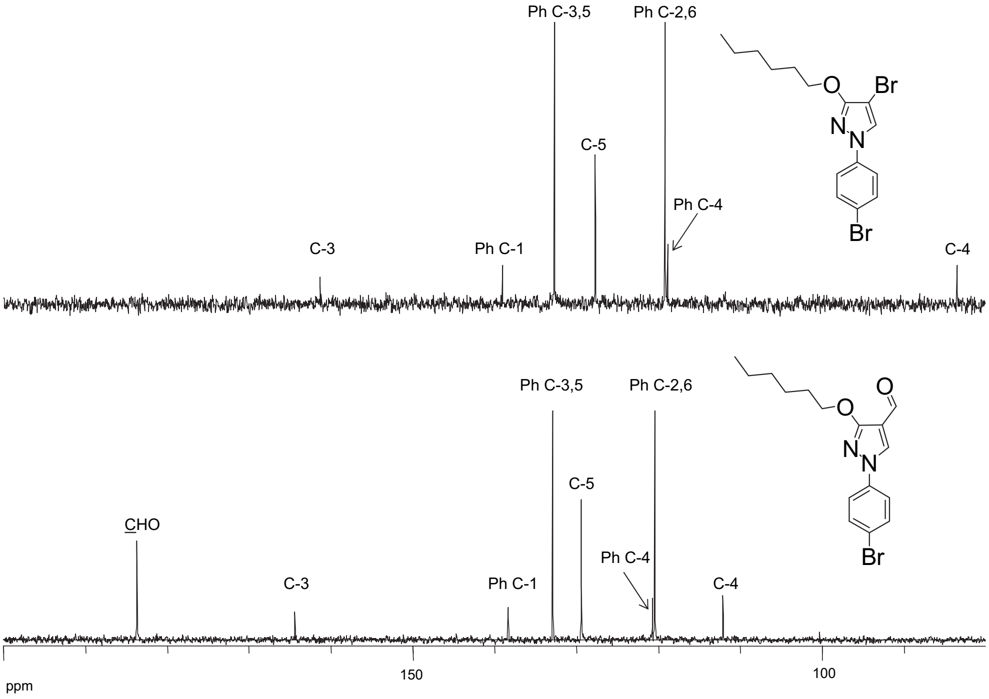

Fig. 1. The aromatic parts of ^{13}C NMR spectral data of compounds **4** (above) and **5** (below) (75 MHz, CDCl$_3$).

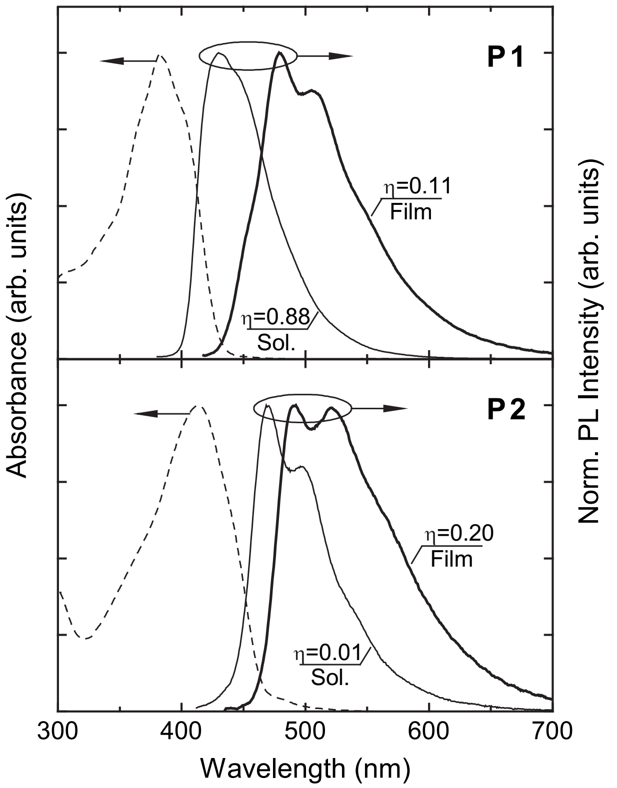

Fig. 2. Absorbance and normalized PL spectra of 10^{-5} M THF solutions (thin lines) as well as PL spectra of thin films (thick lines) of **P1** and **P2**. PL quantum yield (η) values are indicated.

and 413 nm, respectively. Presence of CN- groups in **P2** causes a bathochromic shift of the absorption band as compared to that of cyano-free compound **P1**. The similar shift amounting to 20–30 nm was also observed for CN-PPV oligomers (with cyano groups at α positions), where it was attributed to the electron-withdrawing nature of cyano groups [18]. The PL spectrum of **P1** solution is Stokes shifted by 47 nm in respect of the absorption band and feature high emission quantum yield ($\eta = 0.88$), whereas in the case of compound **P2** bearing cyano groups, Stokes shift is found to be slightly larger (57 nm), and more importantly, a huge decrease in emission quantum yield ($\eta = 0.01$) is observed. Furthermore, high PL quantum yield of the isolated molecules of **P1** in the solution is reduced down to 0.11 (by a factor of 8) in the solid state. In sharp contrast to this, very weak fluorescence of **P2** solution experiences boost in efficiency up to $\eta = 0.20$ (by a factor of 20) upon condensation (Fig. 2).

It is known that cyano groups attached into vinylene linkage with phenyl rings facilitate intramolecular torsions around the vinylene double bonds due to the steric hindrance resulting in fluorescence quenching in the isolated molecules [19]. This is in agreement with our observations of very low η obtained for **P2** in a dilute solution. As opposed to that, the isolated molecules of analogous cyano-free compound **P1** feature coplanar structure, which determines high emission yield of **P1** in a solution.

The reduction of fluorescence efficiency in the solid state is common for majority of fluorophores and is due to excitation migration-related quenching in the solid state. In the film of **P1** the molecule coplanarity enhances exciton coupling, which promotes the nonradiative decay mainly due to excitation migration to intrinsic defects or impurity-related quenching sites [19]. Since the films were prepared in ambient conditions, oxygen is likely to play a significant role in the emission quenching. However, emission enhancement (in the case of **P2**) followed by transition from the liquid to solid phase is untypical and need to be clarified. In a solid state cyano-substituted **P2** molecule torsions and so the torsion induced nonradiative deactivation processes are suppressed due to the rigid environment [19,20]. Moreover, steric and electrostatic effects induced by the introduction of bulky and polar substituents prevent tight packing of the molecules in the solids, what significantly reduces excitation migration, and thus, lowers exciton migration-related quenching. This explains much higher (by a factor of 20) fluorescence efficiency in the films of **P2** as compared to that in solutions and by a factor of two higher efficiency as compared to that of the films of **P1** composed of highly fluorescent planar molecules (see Fig. 2). The enhancement of fluorescence efficiency for the compounds featuring cyano groups in a solid state as compared to that in solution was also reported in numerous papers [8,19,21].

PL transients measured in the dilute solutions and thin films of **P1** and **P2** are depicted in Fig. 3. The solution of **P1** exhibits single exponential decay with decay time constant (τ) of about 0.9 ns. Exponential decay accompanied with close to unity fluorescence quantum yield in planar **P1** molecules clearly indicates the domination of radiative relaxation. The PL decay of **P2** solution is found to be considerably faster ($\tau < 0.1$ ns) as compared to that of **P1**. Since the decay is faster than the instrument response function (IRF), PL transient closely follows the IRF and inhibits more precise estimation of the time constant. Short PL decay time of **P2** in solution is consistent with very low emission yield and evidences the significance of nonradiative relaxation.

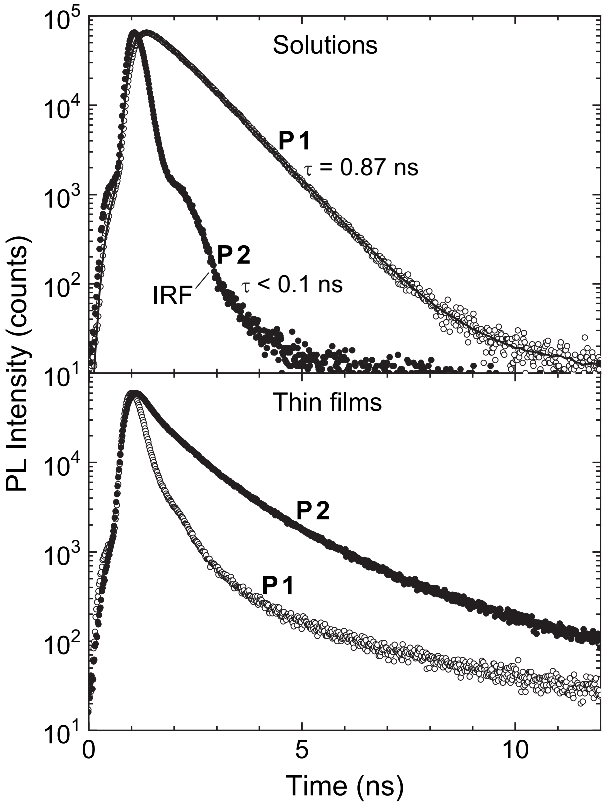

Fig. 3. PL transients of **P1** and **P2** in 10^{-5} M THF solutions and in the thin films (points). Line indicates a single exponential fit to the experimental data. IRF – instrument response function.

The PL transient in the film of **P1** is strongly non-exponential, which is in agreement with migration-related exciton quenching. As opposed to the PL decays in the solutions, the decay of the **P2** film was found to be slower than that of **P1** film and much slower than that of **P2** solution supporting the assumption on suppressed exciton migration and nonradiative deactivation in less tightly packed film of **P2** with cyano groups.

Evidently, the PL transients in the films and solutions qualitatively correlate with the PL quantum yield data pointing out significance of cyano substituents of the pyrazole-based polyconjugated molecules on the excitation deactivation pathways via molecular torsions in a liquid phase or reduction of exciton migration-related quenching in condensed phase.

The ionization potentials of the **P1** and **P2** were found to be 5.46 eV and 5.90 eV, respectively. Assuming the bandgaps of **P1** and **P2** films to be roughly the same (see Fig. 2) the larger I_p value of **P2** achieved upon introduction of cyano groups into the vinylene linkages resulted in the increased electron affinity of **P2** by more than 0.4 eV, as compared to that of **P1**. This is consistent with the higher electron affinities reported for cyano-substituted PPV polymers [7].

Transparent and homogeneous film of **P1** molecularly dispersed in polymer host of bisphenol Z polycarbonate (PC-Z) (with P1 to PC-Z mass ratio of 1:3) was prepared by the casting technique and used in XTOF measurements. Unfortunately, the solubility of the compound **P2** was insufficient to prepare the film of the required thickness for the estimation of charge carrier mobility. Fig. 4 shows the transients of the surface potential decrease rate dU/dt in **P1**: PC-Z film measured at different applied voltages. The transit time t_t of charged carriers was determined from the kink in the dU/dt transient plotted in a double logarithmic scale and then used to deduce the drift mobility (μ) using the formula $\mu = d^2/U_0t_t$, where d is the sample thickness and U_0 is the surface potential at the moment of the excitation.

The room temperature electric field dependence of the hole drift mobility (μ_h) for the solid solution of **P1** in PC-Z is presented in Fig. 5. The exponential increase of μ_h with the square root of the electric field was observed. Such behavior is commonly observed for organic charge transporting materials in amorphous state due to a disorder [12]. μ_h of **P1** dispersed in PC-Z was found to attain the value of 3.5×10^{-7} cm^2 V^{-1} s^{-1} at an electric field of 1 MV cm^{-1}. The obtained μ_h value is considered to be rather moderate as compared to the typical values of μ_h for charge transporting materials dispersed in polymers [22].

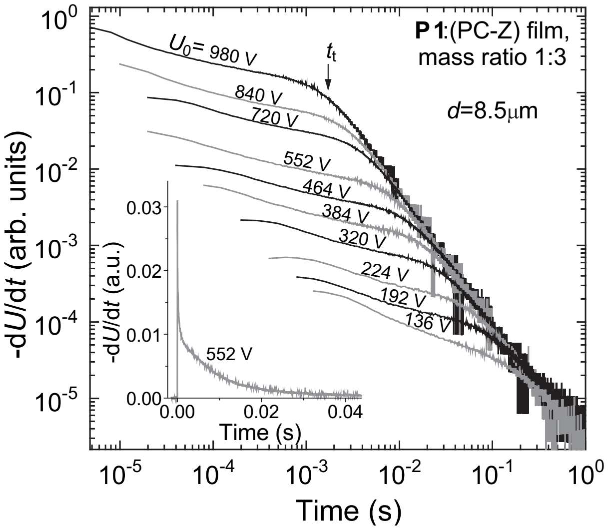

Fig. 4. XTOF transients in a double logarithmic scale for the **P1** dispersed in PC-Z using the mass ratio 1:3. Arrow indicates hole transit time at $U_0 = 980$ V. Inset shows a typical transient curve in a linear scale.

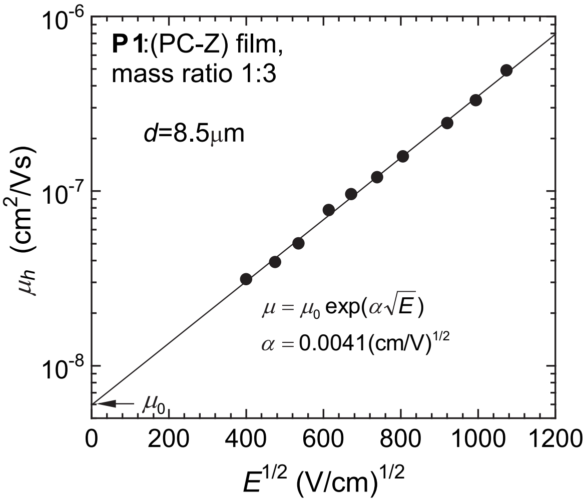

Fig. 5. Hole drift mobility (μ_h) as a function of the square root of electric field for **P1** dispersed in PC-Z (mass ratio 1:3). Line is exponential approximation of the experimental data points. μ_0 - mobility at $E = 0$.

4. Conclusions

Pyrazolyl-substituted diethylene derivative and the analogous compound with the additional cyano groups attached at the vinylene linkages were synthesized and characterized. The ionization potential measurements indicated that introduction of cyano groups into the vinylene linkages increases the I_p from 5.46 eV to 5.90 eV, what in conjuction with PL data also leads to increased electron affinity for pyrazolyl-substituted diethylenes. The hole drift mobility estimated by xerographic time-of-flight technique for the solid solution of cyano-free derivative dispersed in polycarbonate (mass ratio 1:3) was found to be 3.5×10^{-7} cm^2 V^{-1} s^{-1} at an electric field of 1 MV cm^{-1}.

The PL measurements revealed high emission quantum yield ($\eta = 0.88$) of the coplanar structure bearing molecules of the cyano-free pyrazole derivative in a solution and very poor yield ($\eta = 0.01$) of the analogous derivative with cyano groups caused by these groups-induced intramolecular torsions. In the films prepared in ambient conditions, the incorporation of cyano moieties was shown to enhance PL efficiency of the pyrazole-based diethylene derivative from 0.11 to 0.20 (by a factor of two). The enhancement was attributed to the suppression of migration-induced quenching of the excitons at the defects in the less tightly packed films of bulky cyano groups-containing pyrazole derivatives.

Acknowledgements

The research was supported by the Lithuanian State Science and Studies Foundation. We gratefully acknowledge habil. dr. V. Gaidelis for the help in ionization potential measurements.

References

[1] (a) Kim DU, Paik SH, Kim SH, Tsutsui T. Synth Met 2001;123:43;
(b) Kwok CC, Wong MS. Chem Mater 2002;14:3158;
(c) Malinauskas T, Stumbraite J, Getautis V, Gaidelis V, Jankauskas V, Juška G, et al. Dyes Pigm 2009;81:131.
[2] Seo HJ, Park HC, Lee SE, Park JW. Curr Appl Phys 2005;5:209.
[3] Kim BS, Joo S-H, Oh D, Wook Cha S, Choi DS, Lee CE, et al. Synth Met 2004;145:229.

[4] Sigalov M, Ben-Asuly A, Shapiro L, Ellern A, Khodorkovsky V. Tetrahedron Lett 2000;41:8573.
[5] Tamoto N, Adachi C, Nagai K. Chem Mater 1997;9:1077.
[6] (a) Lu Z, Jiang Q, Zhu W, Xie M, Hou Y, Chen X, et al. Synth Met 2000;111–112:465;
(b) Sano T, Fujii Y, Nishio Y, Hamada Y. Jpn J Appl Phys 1995;34:3124;
(c) Zhang XH, Wu SK, Gao ZQ, Lee CS, Lee ST, Kwong HL. Thin Solid Films 2000;371:40.
[7] Greenham NC, Moratti SC, Bradley DDC, Friend RH, Holmes AB. Nature 1993;365:628.
[8] An BK, Kwon SK, Jung SD, Park SY. J Am Chem Soc 2002;124:14410.
[9] Adams MJ, Highfield JG, Kirkbright GF. Anal Chem 1977;49:1850.
[10] Mello JC, Wittmann HF, Friend RH. Adv Mater 1997;9:230.
[11] Miyamoto E, Yamaguchi Y, Yokoyama M. Electrophotography 1989;28:364.
[12] (a) Getautis V, Paliulis O, Paulauskaite I, Gaidelis V, Jankauskas V, Sidaravicius J, et al. J Imag Sci Tech 2004;48:265;
(b) Simokaitiene J, Laukyte D, Grazulevicius JV, Kazlauskas K, Jursenas S, Jankauskas V. Dyes Pigm 2009;81:235.
[13] Montrimas E, Gaidelis V, Pazera A. Lithuanian J Phys 1966;6:569.
[14] Vaezi-Nejad SM. Int J Electronics 1987;62:361.
[15] (a) Harries C, Loth G. Ber Dtsch Chem Ges 1896;29:513;
(b) Nedzelskyte E, Martynaitis V, Sackus A, Eller GA, Holzer W. Molbank 2007;3:M551.
[16] Olkhovik VK, Vasilevskii DA, Pap AA, Kalechyts GV, Matveienko YV, Baran AG, et al. Archivoc 2008;9:69.
[17] Sarker AM, Gürel EE, Ding L, Styche E, Lahti PM, Karasz FE. Synth Met 2003;132:227.
[18] Hanack M. Thin Solid Films 2002;417:26.
[19] Oelkrug D, Tompert A, Egelhaaf H, Hanack M, Steinhuber E, Hohloch M, et al. Synth Met 1996;83:231.
[20] Kim BK, Choi CH, Lee SH, Lee YS, Zong K, Yu SC. Colloids Surf A 2001;180:41.
[21] Palayangoda SS, Cai X, Adhikari RM, Neckers DC. Org Lett 2008;10:281.
[22] (a) Matoliukstyte A, Burbulis E, Grazulevicius JV, Gaidelis V, Jankauskas V. Synth Met 2008;158:462;
(b) Simokaitiene J, Grigalevicius S, Grazulevicius JV, Rutkaite R, Kazlauskas K, Jursenas S, et al. J Optoelectron Adv Mater 2006;8:876.